

DIFFUSION MEASUREMENT FROM TRANSVERSE ECHOES

Y. S. Li*, Carleton College, Northfield, MN, USA

Abstract

Beam diffusion is an important measure of stability in high intensity beams. Traditional methods of diffusion characterization (e.g. beam scraping) can be very time-consuming. In this study, we investigate the transverse beam echo as a novel technique for measuring beam diffusion. Numerical analysis of maximum echo amplitude was compared with theoretical predictions with and without diffusion. We succeeded in performing a self-consistent measurement of diffusion coefficient D_1 via a parameter scan over delay time τ . We also demonstrated the effectiveness of pulsed quadrupoles as a means to boost echo amplitude. Finally, multi-echo sequences were also briefly investigated. Results from this study will support planned experiments at the IOTA proton ring under construction at Fermilab.

INTRODUCTION

A significant barrier to the reliable operation of high intensity beams is beam diffusion due to space charge and other intensity dependent effects. The traditional method of diffusion characterization using beam scraping is a very time-intensive process that could take many hours to complete [1]. In this study, we investigate transverse beam echoes as a novel method to measure diffusion. The echo signal amplitude is extremely sensitive to any phase perturbations and more importantly, requires only several thousand turns to measure. Transverse beam echoes have been primarily observed in proton and heavy-ion rings [2]. The basic elements of an echo are the following: (a) non-linear ring elements (e.g. octupoles) to introduce action-dependence in the betatron frequency, (b) dipole kick to initiate the echo sequence and (c) quadrupole kick after delay time τ . At time 2τ , we will observe spontaneous oscillations in the beam centroid, which is an “echo” of the original dipole kick (Fig. 1). An animation of the echo sequence can be found in [3].

THEORY

Echo Characteristics

If we assume an initial Gaussian beam distribution and linear action-dependence in ω , i.e.

$$\psi_0(J) = \frac{1}{2\pi J_0} e^{-J/J_0}, \quad \omega(J) = \omega_0 + \omega' J, \quad (1)$$

where J_0 is the initial emittance, ω_0 is the base betatron frequency and ω' is the detuning parameter, then the echo amplitude is given analytically by [4, 5]

$$\langle x \rangle_{\text{ampl}}(\xi) = \frac{a}{(1 + \xi^2)^{3/2}}, \quad (2)$$

$$\text{where } a = \theta q \sqrt{\beta \beta_k} \omega' J_0 \tau. \quad (3)$$

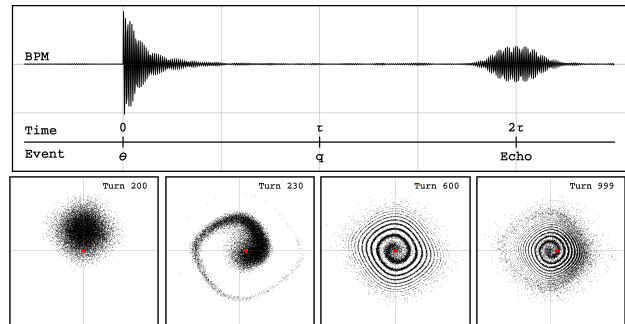


Figure 1: *Top*: Simulated BPM output for a typical echo sequence. *Bottom*: Phase space portraits a) after dipole kick, b) experiencing phase decoherence, c) after quad kick and d) at time of maximum echo amplitude. Red dot indicates beam position centroid.

Here, a is the maximum amplitude of the echo, $\xi \equiv \omega' J_0(t - 2\tau)$ is the normalized time variable and β, β_k are the betatron functions at the BPM and dipole kicker respectively. It is also useful to define the normalized maximum echo amplitude:

$$A = \frac{a}{\sqrt{\beta \beta_k} \theta}. \quad (4)$$

We expect A to have a theoretical limit of 1, since we do not expect to recover more phase information in the echo than was present right after the dipole kick. In practice, saturation effects set in much sooner, as we shall see shortly. It is also important to note that we made two key assumptions in the analysis:

1. The delay time τ is much larger than the decoherence time τ_{decoh} .
2. Both dipole kick θ and quad kick q are weak.

These assumptions impose limits on our working parameter space. A precise mathematical statement of these assumptions can be found in [5].

Diffusion

Beam diffusion is modeled by the eponymous PDE

$$\frac{\partial \psi}{\partial t} = \frac{\partial}{\partial J} \left(D(J) \frac{\partial \psi}{\partial J} \right), \quad (5)$$

$$\text{where } D(J) = D_0 + \sum_n D_n \left(\frac{J}{J_0} \right)^n, \quad n \geq 0. \quad (6)$$

Here, $\psi(J, \phi, t)$ is the beam distribution in phase space. The diffusion coefficient $D(J)$ can contain any number of linear or nonlinear terms. We will assume in this analysis that $n = 1$ (linear). The maximum echo amplitude becomes

* liy@carleton.edu

attenuated with diffusion [5, 6],

$$a_{\text{difn}} = a_0 \left(\frac{\exp(1 - \alpha_0)}{\alpha_1^3} \right), \quad (7)$$

$$\text{where } \alpha_i = 1 + \frac{2}{3} D_i \omega'^2 \tau^3, \quad (8)$$

and a_0 is the unattenuated echo amplitude. Both the exponential dependence on D_0 and inverse cubic dependence on D_1 highlight the sensitivity of the echo amplitude to diffusion. Note that a_{difn} can be maximized with respect to delay time τ and detuning ω' . Assuming D_0 is negligible, we find [6],

$$\tau_{\text{max}} = \left(\frac{16}{3} \omega'^2 D_1 \right)^{-1/3}, \quad \omega'_{\text{max}} = \left(\frac{10}{3} \tau^3 D_1 \right)^{-1/2}, \quad (9)$$

where τ_{max} and ω'_{max} represent the respective ‘‘optimal’’ parameter value for maximum A .

Pulsed Quadrupoles

It is possible for strong diffusion effects to completely attenuate the echo signal. Pulsed quadrupoles is one method to boost echo amplitude in order to counter this. In a pulsed quadrupole sequence, each quad kick is timed in order to reinforce the effect of the preceding kick. Notation wise, we use character sequences to describe the kicks. A one-turn positive kick is indicated with ‘p’, while ‘n’ denotes a negative kick. The absence of a kick is marked with ‘x’. The length of the sequence N_{pulse} is measured in terms of the number of *additional* kicks. Therefore, the sequence pnpn has length 3 and indicates a positive kick at N_τ turns, negative kick at $N_\tau + 1$, positive kick at $N_\tau + 2$, and finally negative kick at $N_\tau + 3$.

SIMULATION

Numerical analysis was performed with an in-house simulation developed in C. The program tracked the phase space Floquet coordinates of individual particles and propagated them along a simulated storage ring (based on RHIC machine parameters [2]) over a preset number of turns. We typically begin with a Gaussian beam distribution. Octupole magnets provided the linear detuning $\omega(J)$. Diffusion, if present, was implemented as random Gaussian dipole kicks θ_R applied at the end of each turn.

RESULTS

Diffusion Measurement

Simulation results from parameter scans over τ and ω' displayed the expected theoretical relationships with echo amplitude (Fig. 2). Furthermore, by estimating τ_{max} we were able to use Eq. (9) to determine the linear diffusion coefficient D_1 .

For Gaussian dipole noise of magnitude $\theta_R = 1 \times 10^{-6}$ rad, we calculated $D_1 = 1.5 \times 10^{-18}$ m-rad²/turn using this method. This was corroborated against a straightforward

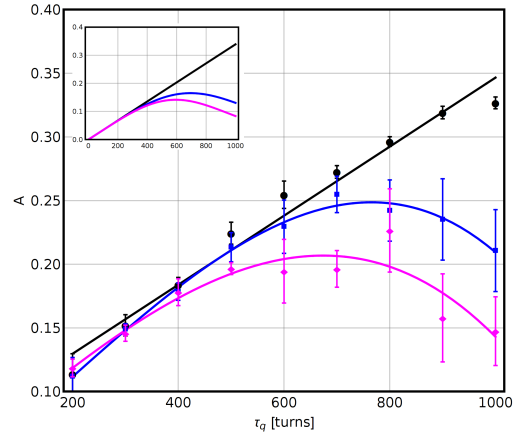


Figure 2: Plot of A versus τ for different values of θ_R . Inset shows theory predictions. By estimating the maxima τ_{max} of the blue and magenta plots, we were able to perform a self-consistent measurement of D_1 .

measurement of D_1 by tracking emittance growth over time. We obtained $D_1 = 1.4 \times 10^{-18}$ m-rad²/turn, which is in excellent agreement with our echo-based estimate. This demonstrates self-consistent results from the simulation.

Pulsed Quadrupoles

Our findings with regards to pulsed quadrupoles can be summarized into four main points.

Pulsed quadrupoles are an effective means to boost echo amplitude, up to saturation. We investigated the dependence of normalized echo amplitude A on the pulse length N_{pulse} using both pn and ppx repetition units (Fig. 3). Starting with an unboosted amplitude of $A_0 = 0.18$, we achieved a maximum amplification factor of nearly 2. This clearly demonstrates the effectiveness of pulsed quadrupoles. However, the echo amplitude is subject to saturation at $A \approx 0.4$. We were unable to surpass this empirical limit regardless of kick strength, length or pattern.

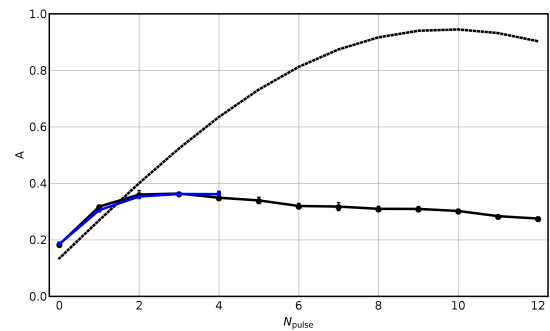


Figure 3: Plot of A versus N_{pulse} for pn (black), ppx (blue) repetition units and theory (black, dotted). Saturation sets in after $N_{\text{pulse}} = 2$ with $A \approx 0.4$.

Optimum pulse sequence is highly dependent on fractional tune. For fractional tunes close to $1/4$ or $3/4$, we found the pn repetition unit to be most effective (Fig. 4). For

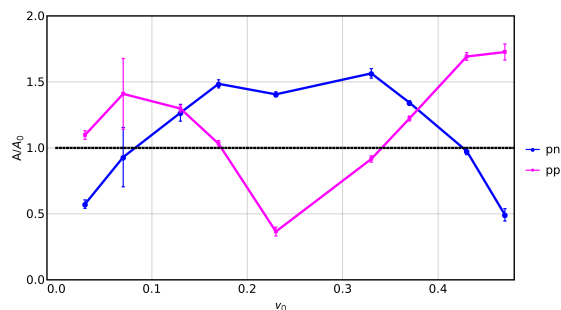


Figure 4: Plot of fractional increase in amplitude A/A_0 versus fractional tune clearly demonstrates the tune-dependence of the optimum kick sequence.

tunes close to integer values or $1/2$, the repeating sequence pp was more suitable. In fact, if an inappropriate sequence was used for the particular tune, it is possible to suppress or completely destroy the echo signal.

pn and ppx repetition units are equivalent. From Fig. 3, we see that the two repetition units are equivalent up to saturation. This is good news, given the current difficulty in building an alternating pn quadrupole of sufficiently high frequency. Note that this substitution works only for tunes close to $1/4$ or $3/4$. However, we expect similar single-polarity units to exist for any fractional tune close to a rational number (e.g. the sequence ‘ppxx’ for tunes close to $1/3$, ‘xxxxppxxx’ close to $1/5$ and so on).

Multi-echo amplification is also possible. Theory predicts additional echoes at $t = 4\tau, 6\tau$ etc. even with a single quadrupole kick (Fig. 5). However, the amplitudes of these secondary echoes are usually much weaker. It is possible to boost the amplitude of the secondary echoes by applying kicks at multiples of τ . In particular, if we apply kicks at τ and 2τ , then the 4τ and 6τ echoes become much more prominent.

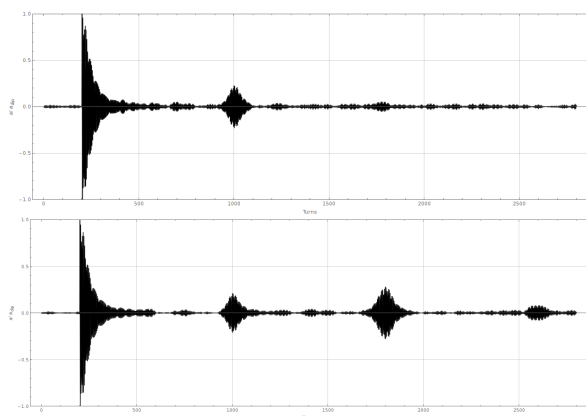


Figure 5: *Top*: Single quad kick at τ giving rise to echoes at 2τ and 4τ . The 6τ echo is not visible. *Bottom*: Quad kicks applied at τ and 2τ . We observe amplification of the 4τ and 6τ echo.

CONCLUSION

To recap the main findings of this study, we were firstly able to perform a self-consistent measurement of the D_1 linear diffusion coefficient using a parameter scan over delay time τ . Next, we investigated various characteristics of the pulsed quad sequence, including its dependence on pulse length, polarity and fractional tune. Finally, we also briefly studied at the amplification of multi-echo sequences.

Saturation remains one of the main barriers to further amplification of the echo signal. Theoretically, saturation arises in the limit where the assumptions of weak q and θ break down. Empirically, we observed saturation to occur near normalized echo amplitude $A \approx 0.4$. Past that point, the singly-peaked echo signal was observed to broaden and eventually split into a weaker doubly-peaked signal.

In addition, multi-echo and pulsed kick sequences still hold a wealth of questions which warrant further investigation. It would also be beneficial to extend the simulation to the full 2D transverse plane, thus accounting for the effects of coupling as well as any other higher order phenomena.

ACKNOWLEDGMENTS

This research project was made possible by the Lee Teng Fellowship in Accelerator Science and Engineering hosted by Fermilab. Additionally, the author would like to thank his research mentor Dr. Tanaji Sen, internship director Dr. Eric Prebys, and the knowledgeable instructors at USPAS for their invaluable guidance and support.

REFERENCES

- [1] G. Valentino *et al.*, *Phys. Rev. ST Accel. Beams* **16**, 021003 (2013).
- [2] W. Fischer, T. Satogata and R. Tomas, in *Proceedings of PAC'05, Knoxville, Tennessee* (IEEE, New York, 2005), pp. 1955-1957.
- [3] A phase space animation of a basic echo (created by the author) can be found at <https://youtu.be/154tM4MBEVI>.
- [4] G. Stupakov, Report No. SSCL-579, (1992).
- [5] A. Chao, *Echoes*, SLAC National Accelerator Laboratory, Lecture Notes.
- [6] T. Sen, *Echoes Notes*, Fermilab (to be published).